Fugu and human may form an important starting point for detecting conserved regulatory elements. We have also identified several sparse conserved segments for most human chromosomes. These segments are tightly linked in *Fugu* but dispersed over whole chromosomes in human. Tracing the fate of such segments in other species may allow us to reconstruct some of the evolutionary history of vertebrate chromosomes.

References and Notes

1. E. S. Lander *et al.*, *Nature* **409**, 860 (2001).
2. J. C. Venter *et al.*, *Science* **291**, 1304 (2001).
3. S. Brenner *et al.*, *Nature* **366**, 265 (1993).
4. R. Hinegardner, *Am. Nat.* **102**, 517 (1968).
5. M. K. Trower *et al.*, *Proc. Natl. Acad. Sci. U.S.A.* **93**, 1366 (1996).
6. K. Gellner, S. Brenner, *Genome Res.* **9**, 251 (1999).
7. S. Baxendale *et al.*, *Nature Genet.* **10**, 67 (1995).
8. B. Venkatesh, S. Brenner, *Gene* **211**, 169 (1998).
9. ———, *Gene* **187**, 211 (1997).
10. O. Coutelle *et al.*, *Gene* **208**, 7 (1998).
11. S. Aparicio *et al.*, *Proc. Natl. Acad. Sci. U.S.A.* **92**, 1684 (1995).
12. B. Venkatesh *et al.*, *Proc. Natl. Acad. Sci. U.S.A.* **94**, 12462 (1997).
13. J. Flint *et al.*, *Hum. Mol. Genet.* **10**, 371 (2001).
14. P. L. Pfeffer *et al.*, *Development* **129**, 307 (2002).
15. W. P. Yu *et al.*, *Oncogene* **20**, 5554 (2001).
16. J. M. Wentworth *et al.*, *Gene* **236**, 315 (1999).
17. D. H. Rowitch *et al.*, *Development* **125**, 2735 (1998).
18. H. Marshall *et al.*, *Nature* **370**, 567 (1994).
19. H. Popperl *et al.*, *Cell* **81**, 1031 (1995).
20. S. Nonchev *et al.*, *Proc. Natl. Acad. Sci. U.S.A.* **93**, 9339 (1996).
21. B. Kammandel *et al.*, *Dev. Biol.* **205**, 79 (1999).
22. L. M. Barton *et al.*, *Proc. Natl. Acad. Sci. U.S.A.* **98**, 6747 (2001).
23. S. Bagheri-Fam *et al.*, *Genomics* **78**, 73 (2001).
24. S. Brenner *et al.*, *Proc. Natl. Acad. Sci. U.S.A.* **99**, 2936 (2002).
25. Supplemental methods and data are available on *Science* Online.
26. C. Fischer *et al.*, *Cytogenet. Cell Genet.* **88**, 50 (2000).
27. T. Hubbard *et al.*, *Nucleic Acids Res.* **30**, 38 (2002).
28. E. Birney, R. Durbin, *Genome Res.* **10**, 547 (2000).
29. EnsEMBL human databases can be accessed at www.ensembl.org.
30. IPI maintains a nonredundant and updated set of human proteins, which can be accessed at www.ebi.ac.uk/IPI.
31. The sequences of these predicted human proteins are available from the project Web sites
32. H. Roest Crollius *et al.*, *Nature Genet.* **25**, 235 (2000).
33. B. Venkatesh, Y. Ning, S. Brenner, *Proc. Natl. Acad. Sci. U.S.A.* **96**, 10267 (1999).
34. These pairings were from the comparative linkage analysis, described in the supplemental material, estimating conserved synteny, which can be accessed at *Science* Online.
35. S. Aparicio *et al.*, data not shown.
36. M. Okabe *et al.*, *Nature* **411**, 94 (2001).
37. A. Yoda, H. Sawa, H. Okano, *Genes Cells* **5**, 885 (2000).
38. W. Wang *et al.*, *Mol. Biol. Evol.* **17**, 1294 (2000).
39. Y. Hirota *et al.*, *Mech. Dev.* **87**, 93 (1999).
40. S. Sakakibara, H. Okano, *J. Neurosci.* **17**, 8300 (1997).
41. M. Okabe *et al.*, *Dev. Neurosci.* **19**, 9 (1997).
42. S. Sakakibara *et al.*, *Dev. Biol.* **176**, 230 (1996).
43. M. Nakamura, H. Okano, J. A. Blendy, C. Montell, *Neuron* **13**, 67 (1994).
44. G. Bernardi, *Gene* **241**, 3 (2000).
45. J. H. Nadeau, D. Sankoff, *Mamm. Genome* **9**, 491 (1998).
46. J. H. Nadeau, B. A. Taylor, *Proc. Natl. Acad. Sci. U.S.A.* **81**, 814 (1984).
47. S. Aparicio, *Nature Genet.* **18**, 301 (1998).
48. J. A. Bailey *et al.*, *Am. J. Hum. Genet.* **70**, 83 (2002).
49. K. H. Wolfe, D. C. Shields, *Nature* **387**, 708 (1997).
50. J. H. Postlethwait *et al.*, *Nature Genet.* **18**, 345 (1998).
51. L. G. Lundin, *Genomics* **16**, 1 (1993).
52. M. Remm *et al.*, *J. Mol. Biol.* **314**, 1041 (2001).
53. S. Aparicio *et al.*, *Nature Genet.* **16**, 79 (1997).
54. A. Amores *et al.*, *Science* **282**, 1711 (1998).
55. S. F. Smith *et al.*, *Genome Res.* **12**, 776 (2002).
56. C. Chothia, A. M. Lesk, *EMBO J.* **5**, 823 (1986).
57. B. Rost, *Protein Eng.* **12**, 85 (1999).
58. We examined the best local identity BLASTP matches from comparing the human proteome with *Fugu*. An expect score threshold of 10^{-2} to 10^{-3} rejects most alignments of <25 to 30% distant protein alignments. It has been previously shown by Chothia, Lesk, Rost, and others that 90% of alignments at or below this "twilight zone" of similarity are unlikely to represent true structural homologies.
59. We found 26,390 of 34,019 matches comparing human peptides with *Fugu* peptides, and a further 687 human peptides that matched *Fugu* assembled sequence or sequence fragments.
60. The accession numbers of these proteins can be accessed at the *Fugu* project Web sites.
61. E. Y. Lee, H. H. Park, Y. T. Kim, T. J. Choi, *Gene* **274**, 237 (2001).
62. A. M. Najakshin, L. V. Mechetina, B. Y. Alabyev, A. V. Taranin, *Eur. J. Immunol.* **29**, 375 (1999).
63. D. B. Lehane, N. McKie, R. G. Russell, I. W. Henderson, *Gen. Comp. Endocrinol.* **114**, 80 (1999).
64. N. Miller *et al.*, *Immunol. Rev.* **166**, 187 (1998).
65. J. L. Grondel, E. G. Harmsen, *Immunology* **52**, 477 (1984).
66. B. R. Peixoto, S. Brenner, *Immunogenetics* **51**, 443 (2000).
67. J. Stenvik, T.O. Jorgensen, *Immunogenetics* **51**, 452 (2000).
68. R. H. Waterston, E. S. Lander, J. E. Sulston, *Proc. Natl. Acad. Sci. U.S.A.* **5**, 5 (2002).
69. E. W. Myers, G. G. Sutton, H. O. Smith, M. D. Adams, J. C. Venter, *Proc. Natl. Acad. Sci. U.S.A.* **99**, 4145 (2002).
70. A. B. Carvalho, A. G. Clark, *Nature* **401**, 344 (1999).
71. Supported by the Agency for Science, Technology and Research, Singapore; the U.S. Department of Energy; and the Molecular Sciences Institute, Berkeley, California. We thank many colleagues and members of our labs for comments on earlier versions of the manuscript.

Supporting Online Material
www.sciencemag.org/cgi/content/full/297/5585/1301/DC1
Sequencing Methods
Supplemental Data
Tables S1 to S7
Figs. S1 to S8
References

21 March 2002; accepted 14 June 2002

REPORTS

Tracing Black Hole Mergers Through Radio Lobe Morphology

David Merritt[1]* and R. D. Ekers[2,3]

Binary supermassive black holes are produced by galactic mergers as the black holes from the two galaxies fall to the center of the merged system and form a bound pair. The two black holes will eventually coalesce in an enormous burst of gravitational radiation. Here we show that the orientation of a black hole's spin axis would change dramatically even in a minor merger, leading to a sudden flip in the direction of any associated jet. We identify the winged or X-type radio sources with galaxies in which this has occurred. The inferred coalescence rate is similar to the overall galaxy merger rate, implying that of the order of one merger event per year could be detected by gravitational wave interferometers.

The detection of gravitational radiation from coalescing supermassive black holes (SBHs) would constitute a rigorous test of general relativity in the strong-field limit (*1*). However, the expected event rate is uncertain because the emission of gravitational waves is negligible until the separation between the SBHs falls below $\sim 10^{-3}$ to 10^{-2} pc. By contrast, simulations of binary SBHs at the centers of galaxies suggest that binary decay may stall at separations of ~ 1 pc, too great for the efficient emission of gravitational waves (*2*). It is unclear whether stellar- or gas-dynamical processes are capable of bridging this gap in a time shorter than the mean time between galaxy mergers. Here we consider whether black hole coalescence can alter the spin axis of the larger black hole and yield a detectable geometric signature in the radio observations of merging galaxies.

We estimate the effect of binary black hole coalescence on the spin of the resulting black hole using angular momentum conservation

$$\mathbf{S}_1 + \mathbf{S}_2 + \mathbf{L}_{\rm orb} = \mathbf{S} + \mathbf{J}_{\rm rad} \qquad (1)$$

where $\mathbf{S}_1$ and $\mathbf{S}_2$ are the spin angular momenta of the two SBHs just before the final plunge,

[1]Department of Physics and Astronomy, Rutgers University, New Brunswick, NJ, 08903, USA. [2]Australia Telescope National Facility, CSIRO, Post Office Box 76, Epping, NSW 2121, Australia. [3]Radio Astronomy Laboratory, 623 Campbell Hall, University of California, Berkeley, CA 94720, USA.

*To whom correspondence should be addressed. E-mail: merritt@physics.rutgers.edu

$\mathbf{L}_{orb}$ is the orbital angular momentum of the binary before the plunge, $\mathbf{S}$ is the spin of the resulting SBH, and $\mathbf{J}_{rad}$ is the angular momentum carried away by the gravitational waves during and after the coalescence. Splitting of the angular momentum as in Eq. 1 is strictly defined only in a post-Newtonian limit (*3*), but this ambiguity is unimportant in what follows.

We denote the masses of the two SBHs as M_1 and M_2, such that $M_1 \geq M_2$, and define their sum as $M \equiv M_1+M_2$. Consider first the effect of the orbital angular momentum on the spin of the resulting black hole. The appropriate value for L_{orb} is the angular momentum of the innermost stable circular orbit (ISCO) of the binary. For $M_2 \ll M_1$, this varies from $\sqrt{12}\ GM_1M_2/c$ (where G is the gravitational constant and c is the speed of light) if the larger SBH is nonrotating to $\sim GM_1M_2/c$ for a prograde orbit around a black hole that spins at the maximum possible rate, $S_1 = GM_1^2/c$ (*4*). When $M_1 \approx M_2$, the ISCO is not easily determined, but various approximations have been derived based on post-Newtonian expansions and numerical calculations.

We estimated the contribution of L_{orb} to the resultant spin in two ways. Adding mass gradually to an initially nonrotating black hole from a fixed plane produces a spin-up that depends solely on the total accreted mass δM; in this limiting case, gravitational radiation losses are negligible and the radius of the ISCO is known precisely (*4*). Alternatively, we can relate S to L_{orb} using the approximate expression (*5*) for the orbital angular momentum at ISCO in unequal-mass black hole binaries; this expression also ignores the gravitational radiation reaction. The two approximations yield similar results (Fig. 1), suggesting that the spin-up of an initially nonrotating black hole will exceed ~1/2 of the maximal spin $S_{max} \equiv GM^2/c$ if the accreted mass exceeds just ~1/5 that of the primary.

Loss of angular momentum by gravitational waves, $\mathbf{J}_{rad}$, becomes increasingly important as M_2 approaches M_1. The fully general-relativistic calculations necessary for computing $\mathbf{J}_{rad}$ have, so far, only been carried out for the case of an equal-mass, circular-orbit binary with no initial spins. Baker *et al.* (*6*) found that about 12% of the system's total angular momentum was carried away by gravitational waves; the final spin was ~0.7 S_{max} (Fig. 1).

We next consider changes in the orientation of the larger black hole's spin axis due to the coalescence. Let ψ be the reorientation angle, i.e., the angle between the initial spin $\mathbf{S}_1$ of the more massive hole and the final spin $\mathbf{S}$. Define $\lambda \equiv \delta S/S_1$, where $\delta\mathbf{S} \equiv \mathbf{S} - \mathbf{S}_1 = \mathbf{L}_{orb} + \mathbf{S}_2 - \mathbf{J}_{rad}$. Then

$$\cos\psi = \frac{1+\lambda\cos\theta}{\sqrt{1+\lambda^2+2\lambda\cos\theta}} \qquad (2)$$

with θ as the angle between $\delta\mathbf{S}$ and $\mathbf{S}_1$. For $\lambda < 1$ the maximum reorientation angle is $\cos\psi_{max} = \sqrt{1-\lambda^2}$, whereas for $\lambda > 1$ any value of ψ is allowed. Assuming a random orientation of $\delta\mathbf{S}$ with respect to $\mathbf{S}_1$ (not strictly justified when $S_1 > 0$, because the radius of the ISCO depends on the relative orientation of $\mathbf{L}_{orb}$ and $\mathbf{S}_1$), the distribution of ψ can be computed and the mean value of $\mu \equiv \cos\psi$ is

$$\langle\mu\rangle = \begin{cases} 1-\dfrac{\lambda^2}{3}, & \lambda\leq 1; \\ \dfrac{2}{3\lambda}, & \lambda>1 \end{cases} \qquad (3)$$

Comparing Eq. 3 with Fig. 1, we conclude that the reorientation angle is expected to be large when $M_2 \gtrsim 0.2\ M_1$, even if the larger hole is rapidly rotating initially. For instance, accretion of a black hole with $M_2 = M_1/4$ results in $\delta S \approx GM_1^2/2c$, comparable to S_1 if the larger black hole's spin is initially ~1/2 of its maximum value. Hence $\lambda \gtrsim 1$ and the reorientation angle could be as large as 180°, with a likely value of ~50°. If the larger black hole is slowly rotating initially, $S_1 \ll GM_1^2/c$, even smaller infalling black holes could produce substantial reorientations; for instance, for $S_1 = 0.1GM_1^2/c$, accretion of a black hole with $M_2 \approx 0.05M_1$ can produce arbitrarily large realignments.

Although the reorientation of a SBH's spin axis due to coalescence is not directly observable, any gaseous accretion onto the SBH is constrained by relativistic frame dragging to be axisymmetric with respect to the black hole (*7*), and it is widely believed that the jets emitted from the centers of active galaxies are launched perpendicularly to the inner accretion disk. Hence, a jet should point in the same direction as the spin axis of the SBH at its center (*8*). The extraordinary long-term stability of the jet direction in many radio galaxies is strong evidence that jet orientations are regulated by black hole spins (*8*, *9*). Because powerful radio galaxies comprise only a fraction (of order 1%) of all bright elliptical galaxies and because radio power is a rapidly increasing function of galaxy luminosity (*10*), we would expect only the more massive of the two merging galaxies to harbor a jet. Therefore, a likely consequence of SBH coalescence in a radio galaxy is a sudden change in the direction of the jet associated with the larger SBH, followed by the generation of a new radio lobe at some (possibly large) angle with respect to the original lobe.

In fact there is a class of radio sources that fit this description: the so-called "winged" or "X-type" radio sources. X-shaped sources are characterized by two low–surface brightness radio lobes (the "wings") oriented at an angle to the "active," or high–surface brightness, lobes (Fig. 2); both sets of lobes pass symmetrically through the center of the associated elliptical galaxy. The first winged source discovered, NGC 326, was initially interpreted by a model in which a single SBH undergoes slow geodetic precession due to torques from an external mass, resulting in an S-shaped radio morphology (*11*); later observations (*12*) revealed the X shape of this source, indicating a more rapid change of jet direction. Other explanations for the origin of X-shaped sources have been proposed, but none has proved satisfactory; black holes are nearly perfect gyroscopes, and reorienting them via external forces is difficult. One proposed model is based on a warping instability of accretion disks (*13*), but this model fails to explain why jet reorientation occurs only once in the X-shaped sources and why most radio galaxies have stable jet directions. Capture of a dwarf galaxy with mass comparable to M_1 could reorient a black hole, but it is more likely that the infalling galaxy would be disrupted by tidal forces before being accreted (*14*).

Seven out of 11 X-shaped radio galaxies in which the length of the wings is at least 80% of the length of the active lobes have Fanaroff-Riley type II (FRII) characteristics; the others are either FRI (NGC 326) or mixed (*15*, *16*) (Table 1). It has been argued that the host galaxies of FRII sources are the products of recent mergers (*17*). Because a major merger of comparably massive galaxies would presumably have induced wiggles in the original jet due to bulk motion of the

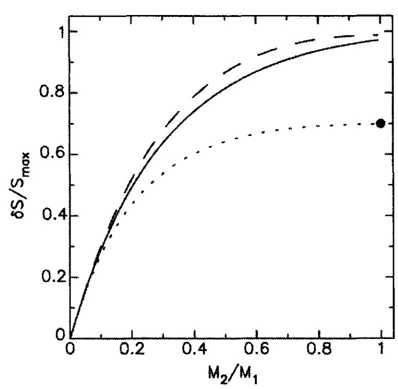

Fig. 1. Spin angular momentum imparted to an initially nonrotating black hole of mass M_1 by accretion of a mass M_2. Accretion is assumed to take place from the ISCO. $S_{max} = G(M_1+M_2)^2/c$, the maximum allowed angular momentum of the resulting hole. Solid line, spin-up produced by the gradual accretion of mass M_2 (*4*); dashed line, spin-up resulting from coalescence with a second hole of mass M_2 (*5*). Both of these curves ignore gravitational radiation losses. The solid circle is from the fully general-relativistic calculation of Baker *et al.* (*6*). The dotted line is a heuristic expression of Wilson and Colbert (*17*) that accounts for gravitational radiation losses, normalized to go through the Baker *et al.* point.

galaxies, the fact that the wings are reasonably straight in most of these sources suggests that the mergers were minor (*18*). This is reasonable because minor mergers far outnumber major mergers and because the infalling SBH [whose mass should scale roughly with host galaxy mass (*19*)] need only have a fraction of the mass of the larger SBH in order to realign it.

The distinctness of the wings and active lobes in the X-shaped galaxies suggests that jet reorientation took place in a relatively short amount of time, $\lesssim 10^7$ years (*20*). In our model, the reorientation of the SBHs occurs almost instantaneously; most of the gravitational radiation accompanying the coalescence of two 10^8 $M_\odot$ SBHs (where $M_\odot$ is the mass of the sun) would be emitted within just ~100 s (*6*). However, the reorientation of the lobe-producing jets would take place on the longer time scale associated with Lense-Thirring precession of the inner accretion disk, $t_{\mathrm{precess}} \sim t_{\mathrm{orb}}(S_{\mathrm{max}}/S)(r/r_s)^{3/2}$, where t_{orb} is the orbital period at radius r and $r_s = 2GM/c^2$ (*17*). The time for reorientation is ~1 year for the inner accretion disk and could be even longer if the continued powering of the jet required a realignment of gas at larger radii. In addition, the second black hole may not find its way to the center of the merged system and form a binary for a long time after the galactic merger. The time scale for infall of the smaller galaxy and its SBH is $\sim 2 \times 10^8$ years $\sigma^5_{200} M_{2,7}^{-3/4}$ where σ_{200} is the velocity dispersion of the larger galaxy in units of 200 km s^{-1} and $M_{2,7} = M_2/10^7\ M_\odot$ (*21*). Hence, we would not necessarily expect to see signs of a recent merger in the morphology of the radio source's host galaxy.

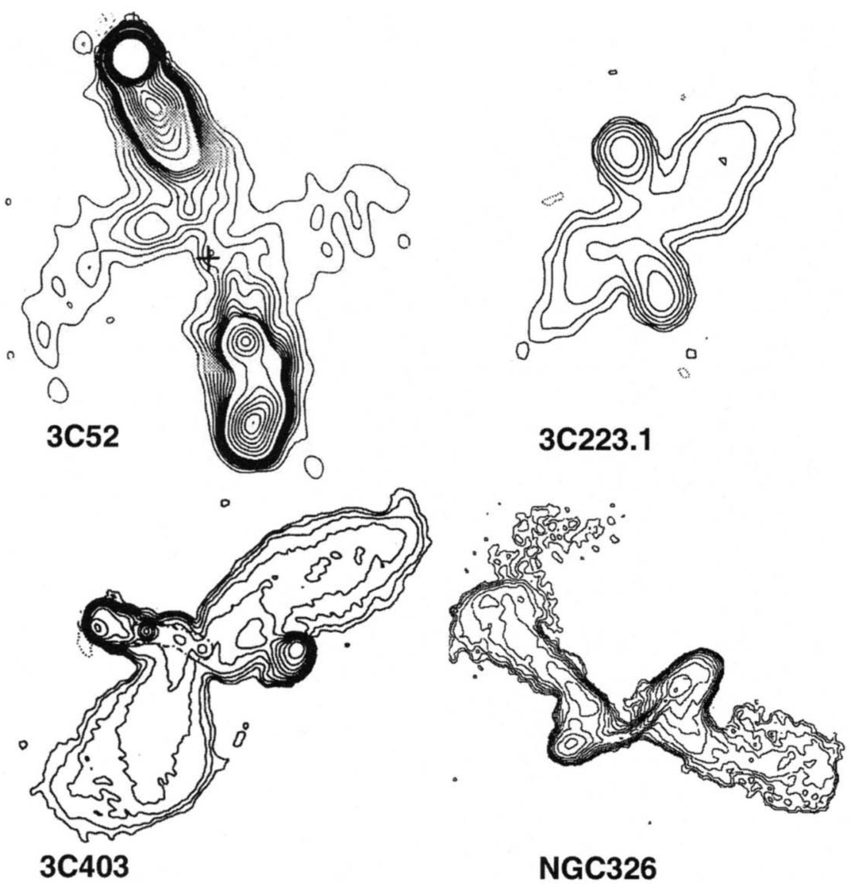

Fig. 2. A composite of four clear examples of the X-shape morphology. VLA radio observations of 3C52 (*28*), 3C223.1 (*29*), 3C403 (*29*), and NGC 326 (*12*).

Table 1. X-shaped radio sources from the compilation of Leahy and Parma (*15*). *z*, redshift; *M*, total visual magnitude of the host galaxy; *T*, estimated time since the relativistic electrons were last accelerated in the wings of the sources; My, million years.

Name	*z*	*M*	*T*	Features
3C52	0.2854	18.5		Dust disk
3C136.1	0.0640	17		Double nucleus or merger remnant
3C223.1	0.1075	16.6	<35 My (*20*)	Dust disk
3C315	0.1083	18.3		Substructure
3C403	0.0590	16.5	<17 My (*20*)	
3C433	0.1016			Dust/star formation
4C12.03	0.1100	17.8		
4C48.29	0.0530	16.0		
B2 0055+26 (NGC 326)	0.0487	13.0	~70 My (*26*)	Double galaxy
B2 0828+32	0.0527	15.1	<75 My (*27*)	
B1059+169 (Abell 1145)	0.0677	15.2		

We speculate that the time scale for accretion disk realignment may influence the radio source morphology. Slow realignment would cause the jet to deposit its energy into a large volume of space, leading to an FRI source with S-type morphology. Rapid realignment would produce an intermediate-luminosity X-shaped source, perhaps with a radio power near the FRI-FRII break. If realignment occurred long ago ($\gtrsim 10^8$ years), the jets and lobes would be well aligned and the source could build up to a high-luminosity FRII source.

The probability of observing a radio galaxy as an X-shaped source in our model is $\sim T_X/T_{\mathrm{merge}}$, where T_X is the length of time that the wings remain visible and T_{merge} is the mean time between mergers. The fading time T_X can be estimated in a number of ways. Table 1 lists estimates of the time since the radiating particles in the wings were last accelerated; if the mean age of the X-sources is in the order of their visible lifetime, the spectral aging estimates in Table 1 imply $T_X \lesssim 10^8$ years. These spectral aging estimates are somewhat model-dependent because of the effects of particle reacceleration, but we can make a direct, semi-empirical estimate of the age by noting the similarity between the wings in the X-sources and the end of the plasma trail in the so-called narrow-angle tail sources found in groups and clusters. Luminosity, spectral shape, polarization, and brightness are similar and, therefore, we would expect both types of source to be visible for a similar time. The galaxies generating these tail sources have velocities typical of the cluster population; we can estimate a dynamical age of $\sim 10^8$ years where the tail fades away (*22*).

If we accept $T_X \approx 10^8$ years and use Leahy and Parma's (*15*) estimate that ~7% of radio galaxies in their sample are X-sources, the mean merger rate for the radio galaxy sample becomes $0.07/10^8$ year ≈ 1 Gy^{-1} (where Gy is billion years). This rate is higher than most estimates of the overall galaxy merger rate, but it should be a fair estimate unless there is a correlation between the presence of the radio source and the population of galaxies undergoing mergers. There are indeed reasons to believe that there may be such a correlation (*23*) and, more speculatively, the black hole coalescence itself may be the trigger for the active galaxy phenomenon. Any such correlation would decrease the implied merger rate for the galaxy population as a whole, but rates of ~ 1 Gy^{-1} are typical of those inferred for galaxies in dense regions or groups (*24*). Our result should motivate more detailed studies of galaxy mergers in the hope of demonstrating that binary SBHs can indeed avoid "stalling" and go on to rapid coalescence.

If the coalescence rate of binary SBHs is comparable to the galaxy merger rate, then the binary separation must be able to drop from ~ 1 to ~ 0.01 pc in a time shorter than ~ 1 Gy. The predicted event rate for gravitational wave interferometers should then be about equal to the integrated galaxy merger rate out to a redshift $z \approx 5$, implying a time between detections of ~ 1 year (*25*).

References and Notes

1. P. L. Bender, in *Gravitational Waves*, I. Ciufolini *et al.*, Eds. (Institute of Physics Publishing, Bristol, UK, 2001), p. 115–133.
2. M. Milosavljevic, D. Merritt, *Astrophys. J.* **563**, 34 (2001).
3. E. E. Flanagan, S. A. Hughes, *Phys. Rev. D* **57**, 4535 (1998).
4. J. M. Bardeen, *Nature* **226**, 64 (1970).
5. L. E. Kidder, C. M. Will, A. G. Wiseman, *Phys. Rev. D* **47**, 3281 (1993).
6. J. Baker, M. Campanelli, C. O. Lousto, R. Takahashi, astro-ph/0202469 (2002).
7. J. M. Bardeen, J. A. Petterson, *Astrophys. J.* **195**, L65 (1975).
8. M. J. Rees, *Nature* **275**, 516 (1978).
9. M. C. Begelman, R. D. Blandford, M. J. Rees, *Rev. Mod. Phys.* **56**, 255 (1984).
10. C. Auriemma *et al.*, *Astron. Astrophys.* **57**, 41 (1977).
11. R. D. Ekers, R. Fanti, C. Lari, P. Parma, *Nature* **276**, 588 (1978).
12. M. Murgia *et al.*, *Astron. Astrophys.* **380**, 102 (2001).
13. J. E. Pringle, *Mon. Not. R. Astron. Soc.* **281**, 357 (1996).
14. D. Merritt, F. Cruz, *Astrophys. J.* **551**, L4a (2001).
15. J. P. Leahy, P. Parma, in *Extragalactic Radio Sources. From Beams to Jets*, J. Roland *et al.*, Eds. (Cambridge Univ. Press, Cambridge, UK, 1992), p. 307–308.
16. The Fanaroff-Riley types I and II are a morphological classification defined by the degree of edge-brightening in the radio lobes [see B. Fanaroff, J. Riley, *Mon. Not. R. Astron. S.* **167**, 31P (1974)].
17. S. Wilson, E. J. M. Colbert, *Astrophys. J.* **438**, 62 (1995).
18. A minor merger is one in which the infalling galaxy has a mass that is 30% or less that of the larger galaxy.
19. D. Merritt, L. Ferrarese, *Mon. Not. R. Astron. Soc.* **320**, L30 (2001).
20. J. Dennett-Thorpe *et al.*, *Mon. Not. R. Astron. Soc.* **330**, 609 (2002).
21. D. Merritt, in *XVth IAP Meeting Dynamics of Galaxies: From the Early Universe to the Present*, Institut d'Astrophysique de Paris, 9 to 13 July 1999, F. Combes *et al.*, Eds. (Astronomical Society of the Pacific, San Francisco, 2000), vol. 197, p. 221–230.
22. C. P. O'Dea, R. N. Owen, *Astron. J.* **90**, 954 (1985).
23. T. M. Heckman et al. *Astrophys. J.* **311**, 526 (1986).
24. R. G. Carlberg et al. *Astrophys. J.* **532**, L1 (2000).
25. M. G. Haehnelt, in *Laser Interferometer Space Antenna*, Jet Propulsion Laboratory, Pasadena, CA, 10 to 15 July 1998, W. M. Folkner, Ed. (American Institute of Physics, Woodbury, NY, 1998), vol. 456, p. 45.
26. M. Murgia, thesis, University of Bologna (2000).
27. U. Klein, K.-H. Mack, L. Gregorini, P. Parma, *Astron. Astrophys.* **303**, 427 (1995).
28. J. P. Leahy, A. G. Williams, *Mon. Not. R. Astron. Soc.* **210**, 929 (1984).
29. J. Dennett-Thorpe, A. H. Bridle, R. A. Laing, P. A. G. Scheuer, *Mon. Not. R. Astron. Soc.* **304**, 27 (1999).
30. P. Leahy kindly allowed us to reproduce the Leahy and Parma catalog of X-shaped radio sources (*15*) in Table 1. We thank him, L. Ferrarese, S. Hughes, M. Milosavljevic, and C. O'Dea for useful discussions. Supported by the NSF through grant 4-21911, NASA through grants 4-21904 and NAG5-8693, and the Miller Institute at the University of California at Berkeley.

4 June 2002; accepted 17 July 2002
Published online 1 August 2002;
10.1126/science.1074688
Include this information when citing this paper.

Current Rectification by Pauli Exclusion in a Weakly Coupled Double Quantum Dot System

K. Ono,[1] D. G. Austing,[2,3] Y. Tokura,[2] S. Tarucha[1,2,4]*

We observe spin blockade due to Pauli exclusion in the tunneling characteristics of a coupled quantum dot system when two same-spin electrons occupy the lowest energy state in each dot. Spin blockade only occurs in one bias direction when there is asymmetry in the electron population of the two dots, leading to current rectification. We induce the collapse of the spin blockade by applying a magnetic field to open up a new spin-triplet current-carrying channel.

Current flow through an electronic system between contact leads (source and drain leads) is determined by the transition rates between the source lead and the drain lead, via states in the electronic system. When inversion symmetry is absent in the system, the electrical current can provide bias-dependent rectification. This was first suggested for a single molecule with appropriately configured molecular orbitals by Aviram and Ratner (*1*) many years ago, and very recently for multiple dots suffering from the Coulomb blockade effect (*2*). In both of these cases, the rectifying effect depends on bias-dependent transition rates and is characterized by irreversible trapping in a state from which current can no longer proceed.

Transition rates in electronic systems depend in general on the Pauli exclusion principle, which prevents two electrons of parallel spin from occupying a single spatial orbital. Observation of the Pauli effect in condensed matter systems depends, however, on low temperatures and reduced dimensions such that the energy spacing of states at the Fermi level is comparable to, or larger than, the thermal energy. One recently observed manifestation of this exchange (i.e., Pauli exclusion) effect in one-dimensional (1D) systems is the suppression of the current noise due to anti-bunching of electrons (*3*, *4*). Here, we show that in transport through a series of 0D sites, with symmetry under inversion appropriately broken, the Pauli effect, in combination with the Coulomb blockade, can be used to block current altogether in one direction while permitting it to flow in the opposite direction, thereby realizing a fully controllable spin-Coulomb rectifier.

Quantum dots are often referred to as artificial atoms because the electrons inside are well confined in 0D states and the electronic properties are analogous to those of real atoms (*5*, *6*). The electronic configuration and the number of electrons in the quantum dot are parameters that can be easily manipulated (*6*–*8*). A quantum dot containing one electron in a single orbital state is just like a hydrogen atom. We use two weakly coupled hydrogen-like quantum dots to construct a diatomic molecule that forms the two-electron two-site system. We can then observe the consequences of Pauli exclusion directly on single-electron tunneling via the two-electron states.

Suppose we have two sites, site 1 and site 2, weakly coupled together, and one electron is permanently localized on site 2 (Fig. 1A). Now consider transport of a second electron through the system between two contact leads. The number of electrons on site 1 (2), N_1 (N_2), varies between 0 and 1 (1 and 2). An

[1]Department of Physics, University of Tokyo, Hongo, Bunkyo-ku, Tokyo 113–0033, Japan. [2]Nippon Telegraph and Telephone Basic Research Laboratories, NTT Corporation, Atsugi-shi, Kanagawa 243–0198, Japan. [3]Institute for Microstructural Sciences M23A, National Research Council of Canada, Ottawa, Ontario K1A 0R6, Canada. [4]Exploratory Research for Advanced Technology Mesoscopic Correlation Project, Japan Science and Technology, Atsugi-shi, Kanagawa 243–0198, Japan.

*To whom correspondence should be addressed. E-mail: tarucha@phys.s.u-tokyo.ac.jp